

Biodiesels from beef tallow/soybean oil/babassu oil blends

Correlation between fluid dynamic properties and TMDSC data

G. A. A. Teixeira · A. S. Maia · I. M. G. Santos ·
A. L. Souza · A. G. Souza · N. Queiroz

CBRATEC7 Conference Special Issue
© Akadémiai Kiadó, Budapest, Hungary 2011

Abstract Cloud point (CP), cold filter plugging point (CFPP), and pour point (PP) of biodiesel samples obtained from blends containing different amounts of beef tallow, babassu oil, and soybean oil were investigated by the corresponding conventional techniques and by temperature modulated differential scanning calorimetry (TMDSC). The CP and CFPP values correlate well with the crystallization temperature (T_{onset}) obtained from the TMDSC curves, being the highest for the biodiesel sample containing the highest amount of methyl stearate. A correspondence between PP and the peak temperature was also noticed, pointing out that pouring ceases after the crystallization of the heavier fatty acid ester. Among the samples of biodiesel, Bio-3 (highest amount of babassu oil) and Bio-4 (highest amount of soybean oil) showed better cold-flow properties, or in other words, lower values of CP, CFPP, and PP. Independently of the composition, the cold-flow properties of all biodiesel samples meet the requirements from the Brazilian National Agency of Petroleum, Natural Gas, and Biofuels (ANP).

Keywords TMDSC · Fluidodynamic properties · Biodiesel · Raw materials blend

Introduction

Biodiesel is mainly produced by the transesterification of vegetable oils and fats via alkaline catalysis, in which the triacylglycerides are converted into fatty acid esters by reaction with an alcohol, usually methanol or ethanol [1–5]. In Brazil, biodiesel is used as a B5 mixture (5 vol.% biodiesel and 95 vol.% conventional diesel), being the soybean oil the main raw material. The continuous rise in the biodiesel percentage added to diesel contributes to the search for alternative sources of raw materials. In this sense, the researches involving the use of blends of vegetable oils and animal fats for the biodiesel production can contribute with new options of raw materials [6, 7].

Aiming at assessing all the aspects of the biodiesel quality, several specifications determine the limits for low-temperature biodiesel tests, such as cloud point, CP, (EN 23 015, ASTM D-2500), pour point, PP, (ASTM D-1997, ASTM D-5949), and cold filter plugging point, CFPP, (EN 116, IP-309, ASTM D-6371) [8].

At low temperatures, biodiesel shows the tendency of partial solidification or loss in fluidity, leading to the interruption of fuel flow and clogging of the filtering system, resulting in poor engine starting. The flow properties at low temperature have been investigated for various biodiesel types and also for esters mixtures found in biodiesel [9–13]. The applicability of biodiesel in cold regions depends on the raw materials used in its synthesis. For example, the cloud point of biodiesel obtained from cheap vegetable oils, such as palm oil, which, due to its high concentration of esters from saturated fatty acids displays a worse behavior at low temperatures, although being more resistant to oxidation, as compared with a biodiesel obtained from oils with a high amount of esters from unsaturated fatty acids [14].

G. A. A. Teixeira · A. S. Maia · I. M. G. Santos ·
A. L. Souza · A. G. Souza · N. Queiroz (✉)
Departamento de Química, Universidade Federal da Paraíba,
CCEN, Cidade Universitária, Campus I, 58059-900 João Pessoa,
PB, Brazil
e-mail: neide@quimica.ufpb.br

Some studies report the improvement in the flow properties at low temperature after a partial crystallization, under controlled conditions, and the removal of components with higher melting points [12, 15–18]. On the other hand, the volume and oxidative stability of biodiesel produced were reduced.

In this work, biodiesel samples were synthesized from different blends of beef tallow, soybean oil, and babassu oil. The products obtained, as well as the corresponding raw materials, had their low-temperature properties characterized by the conventional tests, CP, CFPP, and PP, which were correlated with data obtained from the temperature-modulated differential scanning calorimetry (TMDSC) curves.

Experimental

Biodiesel synthesis

In the synthesis of the biodiesel samples, different amounts of beef tallow, babassu oil, and soybean oil were blended. The mass proportions of beef tallow, soybean oil, and babassu oil were 1:1:1 for the sample of blend MO-1, 2:1:1 for the sample of blend MO-2, 1:2:1 for the sample of blend MO-3 and 1:1:2 for the sample of blend MO-4. The transesterification of the blends with methanol was carried out as previously described [19], with the synthesis of the biodiesel samples named Bio-1, Bio-2, Bio-3, and Bio-4, respectively.

TMDSC

The curves of temperature-modulated differential scanning calorimetry (TMDSC) were performed with 7 mg of sample, under nonisothermal conditions in a TA Instruments, model DSC 2920, in nitrogen atmosphere, at a flow rate of 50 mL min⁻¹. The samples were heated from -60 to 100 °C, with a heating rate of 4 °C min⁻¹ and temperature modulation of ±1 °C, over a period of 40 s. Each sample was run in duplicate.

Cloud point (CP), cold filter plugging point (CFPP), and pour point (PP)

Analysis of cold filter plugging point (CFPP) was performed according to the standard ASTM D 6371, in a Tanaka equipment, model AFP-102. Analyses of pour point (PP) and cloud point (CP) were performed according to the standards ASTM D 14747 and D 6371, respectively, in a Pour Point/Cloud Point Tanaka equipment, model MPC-102L. Each sample was run in duplicate.

Fatty acid profile by GC/MS

The samples from the blends MO-1, MO-2, MO-3, and MO-4, as well as their corresponding biodiesel samples were analyzed in a SHIMADZU model QP 2010 gas chromatograph/mass spectrometer. The separation was performed in a Durabond DB-5HT (30 m × 0.32 mm × 0.10 μm) column. Helium was used as the carrier gas, at a flow rate of 3.0 mL min⁻¹. The column temperature was programmed from 130 to 170 °C (heating rate of 2 °C min⁻¹), followed by an increase to 187 °C (heating rate of 1 °C min⁻¹) and after by an increase to 250 °C (heating rate of 20 °C min⁻¹). Initial and final temperatures were held for 1 and 10 min, respectively. The injector was set at 290 °C and the temperature of the mass detector and interface were set at 250 °C. A sample volume of 1.0 μL was injected using split mode (split ratio of 1:50). The fatty acid methyl esters (FAME's) were identified by comparison of the mass spectra standards of the software library (Mass Spectral Database NIST/EPA/NIH). The fatty acid composition was calculated by the corresponding area and was reported as the relative percentage of the total peak area.

Results

Profile of fatty acid esters in the blends and in the biodiesel samples

Table 1 shows the fatty acid esters composition of the blends and the biodiesel samples. They consist mainly of esters derived from saturated fatty acids, except for the Bio-4 sample.

Temperature-modulated differential scanning calorimetry

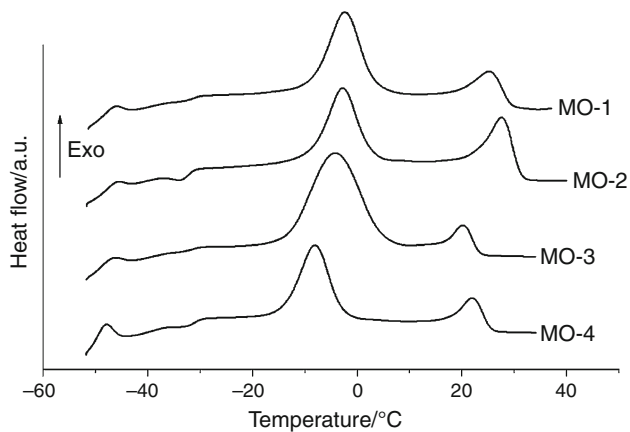
The TMDSC technique was used in this work, once this technique indicates transitions that correspond to melting/crystallization and liquid–liquid transitions. In the TMDSC cooling curves of the blends containing different amounts of beef tallow, babassu oil, and soybean oil mixtures were observed two main exothermic peaks, Fig. 1. The first peak corresponds to the freezing of the least volatile compounds (triacylglycerides containing saturated fatty acids), and the second peak is due to the freezing of most volatile compounds (triacylglycerides containing unsaturated fatty acids).

The fatty acid saturated chains increase the melting point of triglyceride, thus showing a significant effect on the low-temperature properties of the blends. The results showed that the MO-2 blend exhibited the highest

Table 1 Fatty acid esters composition of the blends and biodiesel samples

Esters from the fatty acids	Concentration/%							
	MO-1	MO-2	MO-3	MO-4	Bio-1	Bio-2	Bio-3	Bio-4
Caprylic (C8:0)	0.02	0.83	1.47	1.17	1.78	0.69	2.04	0.90
Capric (C10:0)	1.49	1.24	2.08	1.73	2.14	1.12	2.51	1.10
Lauric (C12:0)	10.24	9.65	15.32	11.14	13.50	10.31	16.31	8.82
Myristic (C14:0)	7.29	6.33	8.61	6.25	8.20	8.08	9.54	5.39
Pentadecanoic (C15:0)	1.16	1.37	0.46	0.54	0.79	1.37	0.57	0.48
Palmitic (C16:0)	16.15	17.73	14.57	14.71	15.19	6.11	14.31	14.37
Palmitoleic [C16:1 (9)]	0.52	0.55	0.35	0.48	0.66	0.86	0.42	0.38
Margaric (C17:0)	2.36	2.54	1.32	1.54	2.49	3.65	1.65	1.44
Stearic (C18:0)	17.74	20.82	14.28	14.12	14.27	24.75	14.69	14.98
Arachidic (C20:0)	0.60	0.62	0.47	0.53	0.43	0.71	0.45	0.54
Behenic (C22:0)	0.44	0.39	0.35	0.46	0.30	0.38	0.28	0.43
Oleic [C18:1 (9)]	20.75	21.06	20.07	20.89	19.86	22.68	19.43	22.27
Linoleic [C18:2 (9,12)]	17.47	14.48	17.62	22.45	16.61	15.87	14.94	24.06
Linolenic [C 18:3 (9,12,15)]	3.26	1.85	2.46	3.99	3.27	3.05	2.53	4.22
Others	0.51	0.54	0.57	0.39	0.51	0.37	0.33	0.62
Saturated	57.49	61.50	58.93	51.80	59.09	57.17	62.35	48.45
Unsaturated	42.00	37.96	40.50	47.81	40.40	42.56	37.32	50.93
Total esters	99.49	99.46	99.43	99.61	99.49	99.63	99.67	99.38

MO blend samples, Bio biodiesel samples

**Fig. 1** TMDSC cooling curves of blends containing beef tallow, babassu oil and soybean oil

crystallization temperature (T_{onset}) of all blends, Table 2. According to the fatty acids profiles of the triacylglycerides (Table 1), this blend displays the highest percentage of stearic acid.

In general, blends with higher peak temperatures (T_{p}) and T_{onset} in the TMDSC cooling curves were the ones with higher proportions of stearic (C18:0) and palmitic acid (C16:0), corresponding to blends MO-1 and MO-2. Regarding the amount of energy involved during the freezing process (exothermic process), the sample MO-2

Table 2 Peak and crystallization temperatures of the studied blends

Sample	$T_{\text{onset}}/^{\circ}\text{C}$	$T_{\text{p}}/^{\circ}\text{C}$	$E_{\text{P1}}/\text{J g}^{-1}$	T_{P2}	$E_{\text{P2}}/\text{J g}^{-1}$
MO-1	29.7 ± 0.1	25.2 ± 0.2	13 ± 0.5	-2.5 ± 0.2	41 ± 0.4
MO-2	31.5 ± 0.2	27.5 ± 0.3	19 ± 0.6	-2.8 ± 0.1	38 ± 0.6
MO-3	23.7 ± 0.1	20.2 ± 0.1	7.1 ± 0.2	-4.2 ± 0.3	66 ± 0.4
MO-4	25.9 ± 0.2	21.9 ± 0.2	9.3 ± 0.2	-8.2 ± 0.1	34 ± 0.5

T_{onset} crystallization temperature, T_{p} peak temperature

released the highest amount of energy (19 J g^{-1}), suggesting to be the one with the biggest degree of molecular organization, Table 2.

The same number of transitions observed in the cooling curves was observed in the heating curves of the blends, but with the endothermic peaks shifting toward higher temperatures. It is believed that preheating eliminated the thermal memory of the blends, by modifying their behavior and did not show transitions in these regions, Fig. 2.

After the transesterification reaction, the entropy of the sample systems increases, because the reduction in the molecules' size occurs an increase in mobility of the molecules. Consequently, the biodiesel samples displayed a higher peak energy than did the corresponding blends, Table 3. The TMDSC cooling curves of the biodiesel samples showed two exothermic peaks, Fig. 3.

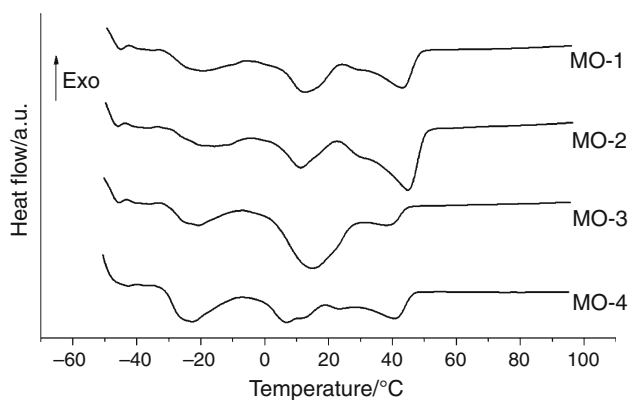


Fig. 2 TMDSC heating curves of tallow, babassu oil and soybean oil blends

Table 3 Peak and crystallization temperatures of biodiesel samples

Sample	$T_{\text{onset}}/^{\circ}\text{C}$	$T_{\text{P1}}/^{\circ}\text{C}$	$E_{\text{P1}}/\text{J g}^{-1}$	$T_{\text{P2}}/^{\circ}\text{C}$	$E_{\text{P2}}/\text{J g}^{-1}$
Bio-1	6.6 ± 0.1	3.03 ± 0.1	44 ± 0.5	-31.8 ± 0.1	32 ± 0.8
Bio-2	10.3 ± 0.2	6.50 ± 0.1	64 ± 0.7	-33.3 ± 0.1	22 ± 0.5
Bio-3	4.8 ± 0.1	-0.03 ± 0.1	29 ± 0.5	-26.7 ± 0.2	28 ± 0.4
Bio-4	4.9 ± 0.1	1.08 ± 0.1	43 ± 0.6	-38.1 ± 0.1	12 ± 0.5

T_{onset} crystallization temperature of the first crystals

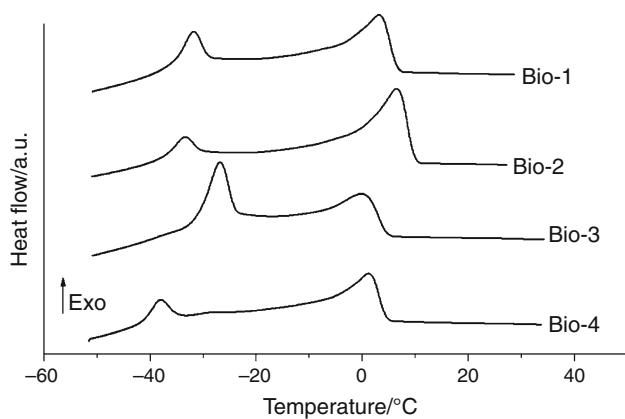


Fig. 3 TMDSC cooling curves of the biodiesel samples

Similar to the behavior of the blends, the biodiesel samples with the highest beef tallow content (Bio-2 and Bio-1), presented also the highest onset and peak temperatures, Table 3. It was evident that the T_{onset} depends mainly on the content of the long and saturated ester chains. However, the peak temperature is related to the content of short and saturated ester chains.

The Bio-3 sample showed a higher concentration of C12:0 than Bio-4, although presenting similar contents of C18:0 and C16:0. Comparing the temperatures of the first exothermic peak for these samples, it is noticed Bio-3

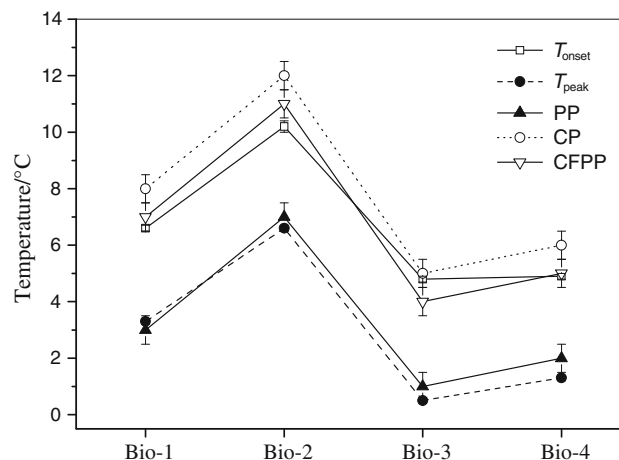


Fig. 4 Correspondence of the values of T_{onset} and peak temperature, obtained from TMDSC curves, with CP, PP, and CFPP

displayed a lower value of T_{P1} than Bio-4. Thus, the crystallization processes began at temperature nearer than room temperature and ended at lower temperatures for the samples with higher content of short and saturated ester chains.

The second exothermic peak was related to the freezing of the fatty acid esters with unsaturated chains, since they have melting points well below the fatty acid esters of saturated chain. The highest concentration of C18:3 in B4 biodiesel sample led to a decrease in the T_{P2} and to the smallest value of the enthalpy E_{P2} , indicating that it is the most organized of the biodiesel sample systems.

The values of T_{onset} and T_{P} , obtained in the TMDSC cooling curves of the biodiesel samples, showed a correspondence with the values of the low-temperature tests, determined by conventional methods, Fig. 4. The values of CP (5–12 °C) and CFPP (4–11 °C) could be correlated with the T_{onset} and were higher for the biodiesel samples with higher contents of methyl stearate. The small differences between the values of CP and CFPP may be related to the size of the crystals, i.e., the appearance of the first crystals was sufficient to hamper the biodiesel flow through the porous medium. This argument is based on the fact that methyl stearate, an ester with a relatively high melting point, in the solid form has long spacings of nearly twice those of ethyl stearate. The amphiphilic nature of methyl stearate molecules causes the formation at low temperatures of bilayered structures with polar carboxylic head-groups aligned head-to-head and next to each other in the crystal interior and oriented away from the nonpolar bulk liquid [20]. It was also noticed a correspondence between PF (1–7 °C) and the peak temperature, indicating that the flow ceases after the heaviest fatty acid esters.

A major problem in the usage of beef tallow use as a raw material for the biodiesel production are its cold-flow

properties. According to the literature, biodiesel made from beef tallow presented a cloud point of 17 °C [21]. In the present work, the use of blend with 50% of beef tallow allowed obtaining a reduction of 5 °C in CP, compared with the biodiesel entirely produced from beef tallow [21]. On the other hand, the biodiesel derived from the blend containing 50% of babassu oil presented lower values of CP, PP, and CFPP, so the presence of babassu oil improved the cold-flow properties of the biodiesel.

The variations in the raw materials' proportions showed that the CFPP, PP, and CP of the biodiesel samples varied significantly. Nevertheless, the low-temperature properties of all biodiesel samples were kept in agreement with the limits established by the ANP Technical Regulation No. 1 from the Resolution number 7, of March 19, 2008.

Conclusions

The production of biodiesel from blends of three raw materials—beef tallow, babassu oil, and soybean oil—gave rise to different cold-flow properties, for the different amounts of these raw materials. The most suitable blend for the production of biodiesel to be used in cold region was the MO-3 sample (50% of babassu oil). Furthermore, the comparison between conventional technique and TMDSC demonstrated that TMDSC was shown to be a useful resource for the study of the cold-flow properties of biodiesel.

Acknowledgements The authors acknowledge the support from the Brazilian agencies: Research and Projects Financing (FINEP), National Council for Technological Development (CNPq) and Coordination for the Improvement of Higher Education Personnel (CAPES).

References

1. Candeia RA, Silva MCD, Carvalho Filho JR, Brasilino MGA, Bicudo TC, Santos IMG, Souza AG. Influence of soybean biodiesel content on basic properties of biodiesel–diesel blends. *Fuel*. 2009;88:738–43.
2. Leung DY, Wu X, Leung MKH. A review on biodiesel production using catalyzed transesterification. *Appl Energy*. 2010; 87:1083–95.
3. Moser BR, Vaughn SF. Coriander seed oil methyl esters as biodiesel fuel: unique fatty acid composition and excellent oxidative stability. *Biomass Bioenerg*. 2010;34:550–8.
4. Predojevic ZJ. The production of biodiesel from waste frying oils: a comparison of different purification steps. *Fuel*. 2008;87: 3522–8.
5. Om Tapanes NC, Aranda DAG, Carneiro JWM, Antunes OAC. Transesterification of *Jatropha curcas* oil glycerides: theoretical and experimental studies of biodiesel reaction. *Fuel*. 2008;87: 2286–95.
6. Taravus S, Temur H, Yartasi A. Alkali-catalyzed biodiesel production from mixtures of sunflower oil and beef tallow. *Energy Fuel*. 2009;23:4112–5.
7. Dias JM, Alvim-Ferraz MCM, Almeida MF. Mixtures of vegetable oils and animal fat for biodiesel production: influence on product composition and quality. *Energy Fuel*. 2008;22:3889–93.
8. Benjumea PN, Agudelo JR, Rios LA. Cold flow properties of palm oil biodiesel. *Revista Facultad de Ingenieria-Universidad de Antioquia*. 2007;42:94–104.
9. Coutinho JAP, Gonçalves M, Pratas MJ, Batista MLS, et al. Measurement and modeling of biodiesel cold-flow properties. *Energy Fuel*. 2010;24:2667–74.
10. Sarin A, Arora R, Singh NP, Sarin R, Malhotra RK, Sarin S. Blends of biodiesels synthesized from non-edible and edible oils: effects on the cold filter plugging point. *Energy Fuel*. 2010;24: 1996–2001.
11. Boros L, Batista MLS, Vaz RV, Figueiredo BR, Fernandes VFS, Costa MC, Krahenbuhl MA, Meirelles AJA, Coutinho JAP. Behavior of mixtures of fatty acid ethyl esters with ethyl stearate. *Energy Fuel*. 2009;23:4625–9.
12. Santos NA, Santos JRJ, Sinfronio FSM, et al. Thermogravimetric and calorimetric evaluation of babassu biodiesel obtained by the methanol route. *J Therm Anal Calorim*. 2009;97:611–4.
13. Imahara H, Minamie E, Saka S. Thermodynamic study on cloud point of biodiesel with its fatty acid composition. *Fuel*. 2006;85: 1666–70.
14. Dunn RO, Bagby MO. Low-temperature properties of triglyceride-based diesel fuels: transesterified methyl esters and petroleum middle distillate/ester blends. *J Am Oil Chem Soc*. 1995;72: 895–904.
15. Santos NA, Tavares MLA, Rosenhaim R, Silva FC, Fernandes VJ Jr, et al. Thermogravimetric and calorimetric evaluation of babassu biodiesel obtained by the methanol route. *J Therm Anal Calorim*. 2007;87:649–52.
16. Dunn RO. Effect of winterization on fuel properties of methyl soyate. In: Peterson CL, editor. *Proceedings of commercialization of biodiesel: producing a quality fuel* Moscow, ID: University of Idaho; 1998. p. 164–86.
17. Gómez MEG, Howard-Hildige R, Leahy JJ, Rice B. Winterization of waste cooking oil methyl ester to improve cold temperature fuel properties. *Fuel*. 2002;81:33–9.
18. Lee I, Johnson LA, Hammond EG. Reducing the crystallization temperature of biodiesel by winterizing methyl soyate. *J Am Oil Chem Soc*. 1996;73:631–6.
19. Baroutian S, Aroua MK, Raman AAA, Sulaiman NMN. Viscosities and densities of binary and ternary blends of palm oil + palm biodiesel + diesel fuel at different temperatures. *J Chem Eng Data*. 2010;55:504–7.
20. Dunn RO. Cold-flow properties of soybean oil fatty acid mono-alkyl ester admixtures. *Energy Fuel*. 2009;23:4082–91.
21. Foglia TA, Nelson LA, Dunn RO, Marmer WN. Low-temperature properties of alkyl esters of tallow and grease. *J Am Oil Chem Soc*. 1997;74:895–904.